

FLUID-STRUCTURE INTERACTION OF TWO-PHASE SCATTERER METAMATERIALS FOR VIBRATION SELF-SUPPRESSION

Wenhan Yuan¹, Yijun Chai¹, Xiongwei Yang¹, Francesco Ripamonti², Xian Wang¹ & Yueming Li¹

¹State Key Laboratory for Strength and Vibration of Mechanical Structures, Shaanxi Key Laboratory of Environment and Control for Flight Vehicle, School of Aerospace Engineering, Xi'an Jiaotong University, Xi'an, 710049, China ²Department of Mechanical Engineering, Politecnico di Milano, Milano 20156, Italy

Abstract

High-end equipment and their service environments often contain numerous flow transfer pipelines, which are critical fluid-solid coupling systems. Unexpected vibrations can lead to poor operational performance and damage the associated devices. This study proposes a novel vibration control method that effectively suppresses low-frequency vibrations by integrating metamaterials with fluid-structure interaction. The self-suppressed vibration of the equipment structure is achieved using the band gaps (BGs) characteristics of the proposed sloshing fluid-structure interaction two-phase metamaterial. The longitudinal dynamic effective mass is analyzed through the energy method, modeling an equivalent impact pendulum, and finite element analysis. This approach reveals the BG distribution mechanism of the sloshing fluid-structure interaction metamaterial. Additionally, the metastructures of unit-cell compositions with varying solid-liquid contact rates are experimentally investigated. The results demonstrate that the proposed technique can effectively create BGs in the low-frequency range by leveraging fluid-structure coupling. Most of the energy is absorbed and scattered through internal solid-liquid interactions during wave propagation. Significantly, by adjusting the solid-liquid contact ratio, the BG of the proposed metamaterial can be enlarged and shifted to the low-frequency band. It provides a straightforward design solution for achieving vibration self-suppression in lightweight fluid-solid structures.

Keywords: Fluid-solid metamaterials, fluid-structure interaction, vibration reduction, low-frequency bandgap

1. Introduction

Many conduits exist in high-end equipment and their service environments, and they are important fluid-structure coupling systems [1][2]. In engineering, the combined effects of fluid, substrate, and aerodynamic excitation loads may lead to structural damage, accuracy degradation, and lifetime reduction [3][4]. Particularly in some extreme cases, including but not limited to extreme temperatures, extreme pressures, and high-speed mechanical motions, pipelines conveying fluids have to meet higher standards of stability and vibration isolation performance[5]. Therefore, the introduction of meta-structures and the use of their unit-cell design of ultra-high degrees of freedom is important for vibration and noise suppression.

In addition, fluid tuning is widely used in the study of band gaps (BGs) tuning of metamaterials due to its high flexibility and low intrinsic frequency. To acquire dynamically tunable vibration isolation performance, however, the major method is to reconfigure the structure by altering the fluid domain parameters inside the metamaterial [6][7][8]. Zhang et al. [6] proposed a fluid-solid coupled elastic (acoustic) metamaterial suitable for low-frequency vibration isolation that exploits the coupling of swift defect modes. The opening and closing of the BG and the adjustment of its position can be achieved by changing the liquid distribution inside the unit cell through a central pump. Wang et al. [9] showed that the BG and transmission properties can be changed by using different liquid inclusions in liquid-solid composite phononic crystals. Wu et al. [10] proposed elastic metamaterials

based on solid-fluid interactions with the internal liquid acting as a scattering core and the outer one being a thin film coating, and the broadband acoustic isolation can be achieved by changing the density of the internal liquid or the thickness of the coating layer to achieve broadband vibration attenuation function. Immediately after, liquid-solid metamaterials with local resonance obtained by using bulging or sloshing design were proposed [11]. In our previous work, a tunable metamaterial with phase change material as scatterer was proposed, whereby the change of the BG can be achieved by a phase change without changing the structure [12]. Previous studies have shown that the fluid-structure interaction of ferromagnetic fluids plays an indispensable role in the BGs of metamaterials [13]. However, there is still a lack of research on the fluid-structure interaction of solid-liquid two-phase coexistence for vibration [14].

Furthermore, the conventional trial-and-error method of materials manufacturing has faced significant issues and formidable challenges due to the growing demand for high performance manufacturing of high-end new materials, integrated and lightweight manufacturing of complex components, and efficient and low-cost green manufacturing of high-end components. The need for lightweight development has led to a great deal of attention being paid to the study of control and sensing integrated in the material in the development of high-end, lightweight equipment [15][16]. Intelligent metamaterials are purposefully designed to sense changes in the environment and respond in a controlled manner, making them valuable in a range of applications including sensors, actuators and adaptive structures [17][18][19]. Consequently, this concept can be applied to prepare a vibration suppression structure based on the material itself by utilizing the destructive fluid-solid interaction.

Thus, fluid-structure interaction of metamaterials is investigated to suppress environmental vibrations, especially the propagation of longitudinal waves. A novel fluid-structure interaction metamaterial filled by solid-liquid two-phase scatterers is proposed. The rest of the paper is organised as follows. Firstly, the mechanism of negative dynamic effective mass generation is analysed using theoretical and numerical methods. Secondly, a parametric study of unit-cell with different solid-liquid contact rates is carried out, and it is proposed that the solid-liquid contact rate and the solid-phase disorder play a joint role in the resonance frequency. Finally, dynamic test experiments are carried out on metastructures with different solid-liquid contact rates to verify the reliability of the parametric study.

2. Model and Methods

2.1 Two-phase Scatterer Interaction Unit-cell

Solid-liquid metamaterials offer significant flexibility in modulating BGs and suppressing vibrations. In this paper, a method for designing metamaterials using fluid-structure interaction sloshing of solid-liquid two-phase scatterers is proposed. The fluid-structure interaction elastic metamaterial consists of a harder external matrix and an internal solid-liquid scatterer. A larger locally resonant BG is produced by the scatterer's fluid-structure interaction effect. The fluid-structure interaction effect of the solid-liquid two-phase of the metamaterial itself can be utilised to regulate the BGs, thus suppressing the vibration. This is conducive to the integration of sensing and control. The metamaterial unit-cell model and the schematic of fluid-structure interaction effect are shown in Figure 1. In this model, the resonator consists of the solid-liquid phases, with the inertial force arising from the solid-liquid phase and the restoring force generated by gravity and solid-liquid interaction.

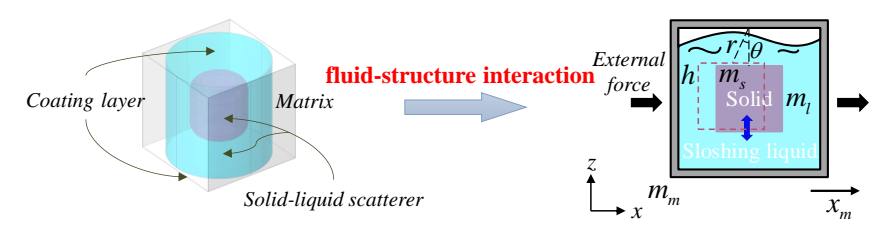


Figure 1 – Schematic diagram of the fluid-structure interaction two-phase metamaterial unit-cell and fluid-structure interaction effect.

2.2 Governing Equations and Dynamic Effective Mass

The mass of the matrix frame is $m_{\scriptscriptstyle m}$ and the solid-liquid phase scatterers are $m_{\scriptscriptstyle s}$ and $m_{\scriptscriptstyle l}$, respectively, as shown in Figure 1. The sloshing of the solid-phase scatterers is expressed in terms of the angle of rotation θ , and r is the radius of rotation. The internal liquid is assumed to be incompressible, inviscid and non-rotating, and there is no cavitation between the liquid and the matrix. Although the unit-cell is 3D, we can use the 2D Laplace equation to describe the motion of the liquid when we are primarily concerned with the first few sloshing modes under this longitudinal loading. The coordinate system used is shown in Figure 1.

First, the Lagrangian function is written as:

$$L = T_m + T_c + T_s + T_l - V_c - V_f - V_s - V_l$$
 (1)

where, T_m is the kinetic energy of the matrix, T_c is the kinetic energy of the coating layer, T_s is the kinetic energy of the solid phase scatterer, and T_l is the kinetic energy of the liquid phase scatterer, V_c is the potential energy of the coating layer, V_f is the external force potential energy, V_s is the shaking potential energy of the solid phase scatterer, and V_l is the potential energy of the liquid phase scatterer force wave.

The height of the free surface is described by velocity potential $\varphi_l(x,z,t)$ and velocity components $v_z(x,z,t)$ [20]. The kinetic energy and potential energy of solid and liquid phase scatterers are as follows:

$$T_{s} = \frac{1}{2} \rho_{s} v_{n} \underbrace{\left\{ \left[\left(\dot{x}_{m} + r_{1} \dot{\theta} \sin \theta \right)^{2} + \left(r_{1} \dot{\theta} \cos \theta \right)^{2} \right] + \dots + \left[\left(\dot{x}_{m} + r_{n} \dot{\theta} \sin \theta \right)^{2} + \left(r_{1} \dot{\theta} \cos \theta \right)^{2} \right] \right\}}_{n}$$
(2)

$$T_{l} = \frac{\rho_{l}}{2} \iint_{\Omega} \left(\left(\frac{\partial \dot{\varphi}_{l}}{\partial x} \right)^{2} + \left(\frac{\partial \dot{\varphi}_{l}}{\partial z} \right)^{2} \right) dx dz$$
 (3)

$$V_{s} = \rho_{s} v_{n} g \underbrace{\left[\left[r_{1} \left(1 - \cos \theta \right) \right] + \dots + \left[r_{n} \left(1 - \cos \theta \right) \right] \right\}}_{n}$$

$$\tag{4}$$

$$V_{l} = \frac{1}{2} \rho_{l} g a \int_{-\frac{a}{2}}^{\frac{a}{2}} \omega(x, t)^{2} dx = \frac{1}{2} \frac{\rho_{l} g a^{2}}{2} q(t)^{2}$$
(5)

where n is the number of solid-phases and define this as the solid-liquid contact ratio. The solid and liquid phase volumes are each half of the scatterer, and assuming that each subsolid volume is equal, then $v_s = nv_n$.

Adopting the small wobble assumption, and the motion of the free surface as:

$$\omega(x,t) = \int_0^t v_z(x,0,\tau)d\tau = q(t)\sin\left(\frac{\pi x}{a}\right)$$
 (6)

velocity potential and velocity components are:

$$\varphi_{l}(x,z,t) = \sum_{n=1}^{\infty} \dot{q}_{n}(t) \sin\left(\frac{n\pi x}{a}\right) \frac{\cosh\left(\frac{n\pi(z+h)}{a}\right)}{\frac{n\pi}{a} \sinh\left(\frac{n\pi h}{a}\right)}$$
(7)

$$v_{z}(x,z,t) = \frac{\partial \varphi_{l}}{\partial z} = \dot{q}(t)\sin\left(\frac{\pi x}{a}\right)f(z)$$
 (8)

where, ρ_s is the density of solid phase scatterer, ρ_l is the density of liquid phase scatterer, a is the lattice constant of the unit-cell, and $\omega(x,t)$ is the height of the free surface. Kinetic energy of the matrix is:

$$T_m = \frac{\rho_m v_m}{2} \dot{x}_m^2 \tag{9}$$

kinetic energy of the coating is:

$$T_c = 2 \iint_S \frac{\rho_c h_c}{2} (\dot{w}_c)^2 dx dz \tag{10}$$

and potential energy of the coating is:

$$V_{b} = 2 \iint_{S} \frac{D_{b}}{2} \left\{ \left(\nabla^{2} w_{b} \right)^{2} - 2 \left(1 - \mu_{m} \right) \left[\frac{\partial^{2} w_{b}}{\partial x^{2}} \frac{\partial^{2} w_{b}}{\partial y^{2}} - \left(\frac{\partial^{2} w_{b}}{\partial x \partial y} \right)^{2} \right] \right\} dx dz$$

$$(11)$$

Assuming a harmonic excitation, the external potential energy:

$$V_f = -F\sin(\omega t)x_m \tag{12}$$

The coupling conditions include the coupling between the liquid phase scatterer and the matrix, as well as the solid-liquid phase coupling of the scatterer. Coupling surfaces of liquid-phase scatterers and matrix is:

$$\frac{\partial \varphi_l}{\partial z} = w_c \left(z = \pm \frac{a}{2} \right) \tag{13}$$

$$\frac{\partial \varphi_l}{\partial x} = 0 \ (x = 0, l) \tag{14}$$

the scatterer solid-liquid phase coupling is:

$$r\dot{\theta}\cos\theta = \frac{\partial\varphi_l}{\partial z} \tag{15}$$

$$r\dot{\theta}\sin\theta = \frac{\partial\varphi_l}{\partial x} \tag{16}$$

Temperature of fluids and solids, heat flow of fluids and solids are equal, respectively.

The two-phase scatterer metamaterial is subjected to external forces, internal solid-liquid coupling and other factors during vibration. With an external force \bar{F} , the forced vibration equation in frequency domain is:

$$\left\{ \left[K_{u} \right] - \omega^{2} \left[M_{u} \right] \right\} \left\{ \overline{x}_{m}, \overline{x}_{T}, \overline{\theta} \right\}^{T} = \left\{ \overline{F}, 0, 0 \right\}^{T}$$

$$(17)$$

and the longitudinal dynamic effective mass:

$$m_{eff} = \frac{F(t)}{\ddot{x}} = \frac{\overline{F}}{-\omega^2 \overline{x}_m} \tag{18}$$

Then, a tuned liquid-mass pendulum impact model with adjustable stiffness is developed based on the mathematical model to predict the dynamic effective parameters. The unit-cell of a conventional locally resonant metamaterial could be analogized to a mass-spring model, where the inertial force of the oscillator is transmitted to the matrix via a spring. However, in the case of the proposed tuned pendulum model with adjustable stiffness, the inertial force (sloshing) of the internal solid is imposed on the matrix through the inertia of the liquid. The plate is not responsible for transmitting this force. Therefore, it is not reasonable to use a conventional mass model to represent a fluid-structure

interaction unit-cell. As shown in Figure 2, the solid-phase scatterer (purple domain) is equivalent to a pendulum ball m_s with a pendulum length r_s . The liquid-phase scatterer (blue domain) is equivalent to a mass block m_l , and the matrix is equivalent to m_m . The solid-liquid interaction is described in terms of the pendulum length r_s and pendulum angle θ . The scatterer is connected to the matrix by two springs, described by k_T . The change in displacement of k_T is x_T and the matrix displacement is x_m .

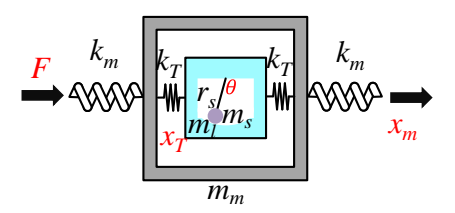


Figure 2 – The equivalent physical model of tuned liquid-mass pendulum impact with adjustable stiffness.

Using the energy method, its dynamic effective mass could be derived. The kinetic and potential energies of the unti-cell shown in Figure 2 are as follows:

$$T = \frac{1}{2} m_{m} \dot{x}_{m}^{2} + \frac{1}{2} m_{l} \dot{x}_{T}^{2} + \frac{2}{3} \left(m_{1} r_{1}^{2} \dot{\theta}_{1}^{2} + \dots + m_{n} r_{n}^{2} \dot{\theta}_{n}^{2} \right)$$

$$+ \frac{1}{2} m_{n} \left\{ \left[\left(\dot{x}_{T}^{2} + \left(r_{1} \dot{\theta}_{1} \cos \theta_{1} \right)^{2} + \left(r_{1} \dot{\theta}_{1} \sin \theta_{1} \right)^{2} \right) \right] + \dots + \left[\left(\dot{x}_{T}^{2} + \left(r_{n} \dot{\theta}_{n} \cos \theta_{n} \right)^{2} + \left(r_{n} \dot{\theta}_{n} \sin \theta_{n} \right)^{2} \right) \right] \right\}$$

$$(19)$$

$$V = k_m x_m^2 + k_T (x_m - x_T)^2 + m_n g \left[r_1 (1 - \cos \theta_1) + \dots + r_n (1 - \cos \theta_n) \right]$$
 (20)

The unit-cell system contains 3 degrees of freedom $q_i = \begin{bmatrix} x_m, & x_T, & \theta \end{bmatrix}^T$ and the Lagrange's equations is:

$$\frac{d}{dt}\frac{\partial L(x_m, x_T, \theta)}{\partial \dot{q}_i} - \frac{\partial L(x_m, x_T, \theta)}{\partial q_i} = 0$$
(21)

where L=T-V. Furthermore, assuming a small wobble, i.e.: $\cos\theta=1$ and $\sin\theta=\theta$. The linear vibration control equation could be obtained.

M and K are the total mass and total stiffness matrices respectively. The dynamic effective mass expression is as follows:

$$m_{eff} = -\frac{1}{\omega^2 \left[-\omega^2 \mathbf{M} + \mathbf{K} \right]^{-1}}$$
 (22)

The exact expression could be calculated by Matlab.

2.3 Experimental Setup and Test Method

A metastructure consisting of eight unit-cell is fabricated using 3D printing additive manufacturing. The preparation of the specimens and the experimental platform are shown schematically in Figure 3. The degree of fragmentation of the solid-phase scatterers is varied to achieve different contact rates while maintaining the same volume of the solid-liquid phase. A signal generator is used to produce sine swept signals in the frequency range of 10.0 Hz to 1000.0 Hz in 500 Hz/s. The acoustic excitation signal is then fed into a shaker connected to the free edge and amplified by a power amplifier to vibrate the specimen. The free edge is fitted with two unidirectional acceleration sensors (sensor A and sensor B) which convert longitudinal structural vibrations into electrical impulses. The shaker input signals and sensor output signals are collected by the LMS SCADA data acquisition system.



- (a) Design of 8 unit-cell metastructures with different solid-liquid contact rates
- (b) Vibration transmission experimental platform

Figure 3 – Preparation and experimental platform for two-phase scatterer metastructures.

3. Result and Discussions

3.1 Verification of Dynamic Characteristics

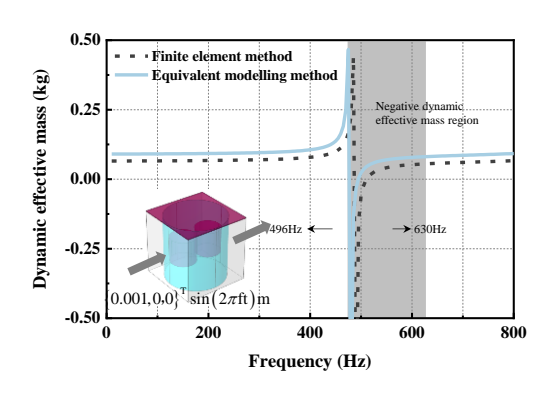
Finite element simulations are used to calculate the effective mass of the fluid-structure interaction two-phase unit-cell. Under the assumption that the sloshing is small and the frequency is low, the elastic vibrations of the solid vessel and the solid and liquid inside are negligible. Therefore, the pressure acoustics module in COMSOL is used to simulate the motion of the liquid. The solid mechanics module is used for the structural region. The acoustic-structural boundary is used for acoustic-solid coupling. The properties of the host structure, filled with solids and liquids, are shown in Table 1.

Table 1. Material parameters of the fluid-structure interaction two-phase unit-cell.

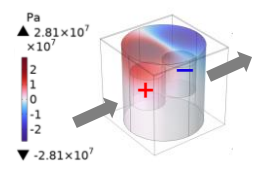
Parameters	Nylon	PI	Liquid paraffin	Solid paraffin
Bulk modulus / (GPa)	1.4	2.4	1.66	0.02
Density / ($kg \cdot m^{-3}$)	1120	1420	850	780
Poisson's ratio	0.3	0.37	0.46	0.40

Figure 4(a) presents the longitudinal effective mass derived from both the finite element simulation and the results of Equation (22). Achieving such a low-frequency BG using conventional solid metamaterials would necessitate either an ultra-slim microstructure or an ultra-heavy scatterer. In contrast, the proposed two-phase scatterer fluid-structure interaction metamaterial leverages the gravitational potential energy of both the liquid and the solid scatterer. The presence of the solid suspension increases the potential energy compared to a purely liquid-filled resonator, making the system more efficient for low-frequency BG formation.

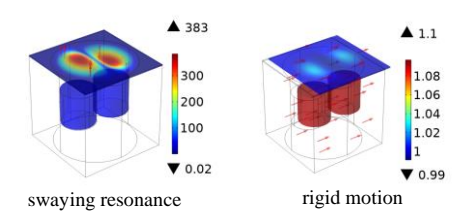
As shown in Figure 4(b), the direction of hydrodynamic forces can be found to be opposite to the direction of the applied displacement load at slightly above the resonance frequency. Meanwhile, Figure 4(c) shows that unlike the rigid displacement at low frequencies, there is an equilibrium stabilisation of the solid-phase scatterer in the negative effective mass region. This is an intrinsic cause of negative mass production, externally reflected in abrupt changes in apparent mass.



(a) FE and equivalent modelling results for longitudinal effective mass



(b) Liquid-phase scatterers at pressures slightly above the resonance frequency



(c) Slightly above resonance and below resonance displacement distributions

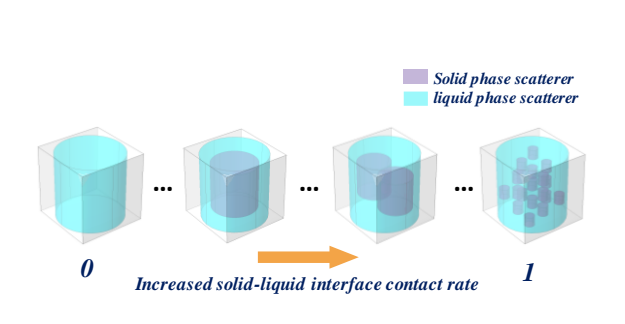
Figure 4 – Longitudinal effective mass of fluid-structure interaction unit-cell, and pressure and displacement near resonance.

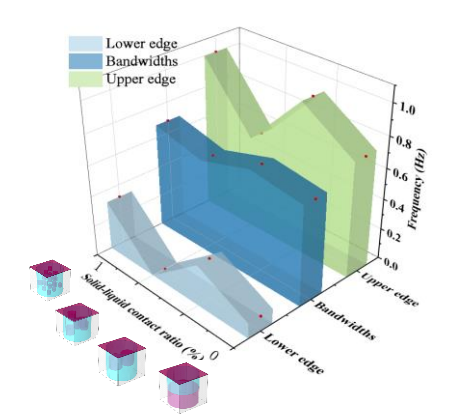
The kinetic and potential energy of the entire solid-liquid scatterer confers a low-frequency BG to the fluid-structure interaction unit-cell. However, as can be seen in Figure 4, the first local resonance interval of the fluid-structure interaction two-phase unit-cell is 496-630 Hz. One possible way to increase the BG is to cascade the unit-cell with different solid-liquid contact ratios, which will be discussed experimentally in Section 3.2.

3.2 Parametric Studies and Harmonic Response of Metastructures

In this section, the negative mass range of fluid-structure interaction two-phase metamaterial unitcell is parametrically investigated and experimentally validated by varying the internal solid-liquid contact ratio.

The poles and zeros of the effective mass, corresponding to the lower and upper edges of the negative mass range, can be derived using Eq. (22). Figure 5(a) illustrates the variation in the ideal solid-liquid contact ratio, ranging from 0 to 1. A solid-liquid contact rate of 0 is defined when there is no solid phase in the scatterer, and as the fractional dispersion of the solid-phase filler increases, the solid-liquid contact rate approaches 1. Figure 5(b) depicts the variation in the band gap (BG) range for several typical contact rates. With a constant volume/mass of the solid phase, the frequency at the upper and lower edges of the negative mass range increases when the sloshing effect is introduced. However, as the solid-liquid contact rate increases, the frequencies at the upper and lower edges first decrease and then increase. This is due to the fact that at constant total mass/volume, the increase in solid fragmentation (n) causes the kinetic and potential energy of the solid phase to keep changing, as shown in Eq. (2) and (4) or Eq. (19) and (20). For this model, the solid-phase scatterer acts not only as the mass of the resonator, but also as a secondary mass hedging the liquid phase of the primary. It is also worth noting that the resonance frequency of a unitcell with half solid-liquid contact rate is close to that of a fixed mass block. Therefore, if a very low frequency BG is obtained through the solid-liquid contact rate, there will be a moderate solid-liquid contact rate. Otherwise, the solid-phase disorder will weaken the liquid-phase spring action, i.e., reduce the kinetic and potential energy of the liquid phase.





(a) Solid-liquid contact ratio by degree of solidphase fractional dispersion

(b) Relationship between the upper and lower edges and bandwidth of the negative mass region with solid-liquid contact rate

Figure 5 – BG and solid-liquid phase contact rates of fluid-structure interaction two-phase metamaterials

Then, the role of the solid-liquid contact rate on the BG is verified by the harmonic response experiments of the metastructure. The metastructure consists of 8 unit-cell with different solid-liquid contact rates. Details of the experiments are given in Section 2.3.

When the metastructure is periodic and each unit-cell is filled with fixed solid, single solid, multiple solids and fragmented solids, the BGs are in the ranges of 240-540 Hz, 300-693 Hz, 192-393 Hz and 295-670 Hz, respectively, as shown in Figure 6. The attenuation range shows a tendency of increasing, then decreasing, and then increasing, which corresponds to the previous results and

verifies the perturbing effect of solid-phase disorder on the liquid-phase resonance. The negative mass interval of the fluid-structure interaction unit-cell is narrow (see Figure 4(a)), and the bandwidth of the transmission valley of the periodic fluid-structure interaction metastructure is relatively wide. It is worth noting that the lower the BG at lower frequencies, the smaller the bandwidth. The desired value can thus be achieved by modulation of the solid-liquid contact rate and solid-phase disorder. Here, it is demonstrated that it is possible to widen the transmission valley by changing the solid-liquid contact rate.

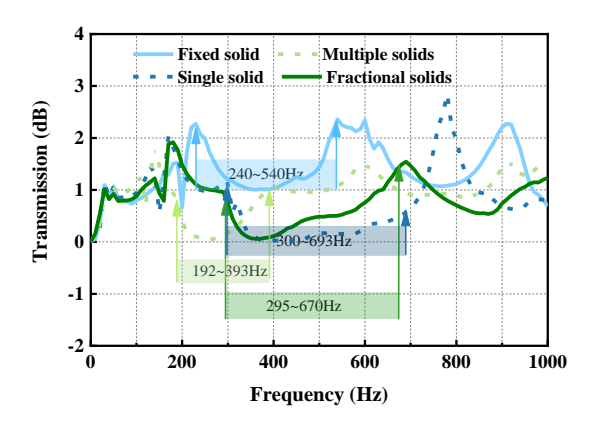


Figure 6 – Longitudinal displacement transmission curves of fluid-structure interaction two-phase metastructures with different solid-liquid contact ratios.

4. Conclusions

In this study, we explore fluid-structure interaction vibrations and propose metamaterials for solid-liquid two-phase scatterers, specifically targeting elastic longitudinal waves. We develop a theoretical model along with an equivalent tuned liquid-mass pendulum impact model to represent the sloshing fluid-structure interaction unit-cell. The longitudinal dynamic effective mass of the proposed unit-cell is calculated, with analytical results showing strong agreement with numerical simulations. The proposed fluid-structure interaction two-phase metamaterial effectively integrates sensing and response mechanisms to attenuate longitudinal waves at very low frequencies. Experimental verification demonstrates that the local resonance frequency and bandwidth can be tuned by adjusting the solid-liquid contact rate and the degree of solid disorder within the filler. This concept has the potential to be extended to other multi-physics metamaterials.

5. Contact Author Email Address

Yueming Li: liyueming@mail.xjtu.edu.cn

Francesco Ripamonti: francesco.ripamonti@polimi.it

6. Copyright Statement

The authors confirm that they, and/or their company or organization, hold copyright on all of the original material included in this paper. The authors also confirm that they have obtained permission, from the copyright holder of any third party material included in this paper, to publish it as part of their paper. The authors confirm that they give permission, or have obtained permission from the copyright holder of this paper, for the publication and distribution of this paper as part of the ICAS proceedings or as individual off-prints from the proceedings.

References

- [1] Guo X, Gao P, Ma H, et al. Vibration characteristics analysis of fluid-conveying pipes concurrently subjected to base excitation and pulsation excitation. *Mechanical Systems and Signal Processing*, Vol. 567, No. 189, pp 110086, 2023.
- [2] Gao P, Yu T, Zhang Y, et al. Vibration analysis and control technologies of hydraulic pipeline system in aircraft: A review. *Chinese Journal of Aeronautics*, Vol. 34, No. 4, pp 83-114, 2021.
- [3] Ding H, Ji J, Chen L-Q. Nonlinear vibration isolation for fluid-conveying pipes using quasi-zero stiffness characteristics. *Mechanical Systems and Signal Processing*, Vol. 121, pp 675-688, 2019.
- [4] Guo X, Cao Y, Ma H, et al. Vibration analysis for a parallel fluid-filled pipelines-casing model considering casing flexibility. *International Journal of Mechanical Sciences*, Vol. 231, pp 107606, 2022.

- [5] Ji W H, Sun W, Zhang Y, et al. Parametric model order reduction and vibration analysis of pipeline system based on adaptive dynamic substructure method. *Structures*, Vol. 50, pp 689-706, 2023.
- [6] Zhang Q, Zhang K, Hu G K. Tunable fluid-solid metamaterials for manipulation of elastic wave propagation in broad frequency range. *Applied Physics Letters*, Vol. 112, No. 22, pp 221906.1-221906.4, 2018.
- [7] Wang T T, Wang Y F, Wang Y S, Laude Vincent. Tunable fluid-filled phononic metastrip. *Applied Physics Letters*, Vol. 111, No. 4, pp 041906, 2018.
- [8] Ge X, Xiang H, Liu Y, et al. Utilizing reversible solid-liquid phase transition to tune phononic bandgaps. *AIP Advances*, Vol. 11, No. 12, pp 125323, 2021.
- [9] Wang Y F. Wang T T, et al. Reconfigurable Phononic-Crystal Circuits Formed by Coupled Acoustoelastic Resonators. *Physical Review Applied*, Vol. 8, No. 1, pp 014006, 2017.
- [10]Wu L, Geng Q, Li Y M. A locally resonant elastic metamaterial based on coupled vibration of internal liquid and coating layer. *Journal of Sound and Vibration*, Vol. 468, pp 115102, 2020.
- [11]Wu L, Li Y M. Harnessing bulging or sloshing modes to design locally resonant liquid-solid metamaterials. *Journal of Sound and Vibration*, Vol. 510, pp 116280, 2021.
- [12]Yuan W H, Chai Y J, Yang X W, et al. Bandgap evolution of metamaterials with continuous solid–liquid phase change. *Journal of Physics D: Applied Physics*, Vol. 56, No. 5, pp 055105, 2023.
- [13]Song Y, Shen Y. Highly morphing and reconfigurable fluid—solid interactive metamaterials for tunable ultrasonic guided wave control. *Applied Physics Letters*, Vol. 121, No. 26, pp 264102, 2022.
- [14]Yi Z, Zhang Z, Huang J, et al. Mechanism analysis and experimental verification of the bulging vibration characteristic of a fluid-solid metamaterial. *Engineering Structures*, Vol. 279, pp 115602, 2023.
- [15]Sun B, Shu D, Fu H, et al. Intelligent Manufacturing for High-End New Materials: Opportunities and Directions. *Strategic Study of CAE*, Vol. 25, No. 3, pp 152-160, 2023.
- [16] Chen Y, Zhang J et al. Intelligent methods for optimization design of lightweight fiber-reinforced composite structures: A review and the state of the art. *Frontiers in Materials*, Vol. 10, pp 1125328, 2023.
- [17]Kirchhof J N, Weinel K, et al. Tunable graphene phononic crystal. *Nano Letters*, Vol. 21, No. 5, pp 2174-2182, 2021.
- [18]Wu, Bin, and Michel Destrade. Wrinkling of soft magneto-active plates. *International Journal of Solids and Structures*, Vol. 208, pp 13-30, 2021.
- [19]Wang Y, Sha W et al. Deep Learning Enabled Intelligent Design of Thermal Metamaterials. *Advanced Materials*, Vol.35, No.33, pp 2302387, 2023.
- [20] Ibrahim R A. Liquid sloshing dynamics: theory and applications. Cambridge University Press, 2005.